

# First-principle derivation of gain in high-index-contrast waveguides

Jacob T. Robinson<sup>1</sup>, Kyle Preston<sup>1</sup>, Oskar Painter<sup>2</sup>, and Michal Lipson<sup>\*1</sup>

<sup>1</sup>Department of Electrical and Computer Engineering, Cornell University Ithaca, NY 14853

<sup>2</sup>Thomas J. Watson, Sr., Laboratory of Applied Physics, California Institute of Technology, Pasadena, California 91125, USA

\*Corresponding author: [ml292@cornell.edu](mailto:ml292@cornell.edu)

**Abstract:** From first principles we develop figures of merit to determine the gain experienced by the guided mode and the lasing threshold for devices based on high-index-contrast waveguides. We show that as opposed to low-index-contrast systems, this quantity is not equivalent to the power confinement since in high-index-contrast structures the electric and magnetic field distributions cannot be related by proportionality constant. We show that with a slot waveguide configuration it is possible to achieve more gain than one would expect based on the power confinement in the gain media. Using the figures of merit presented here we optimize a slot waveguide geometry to achieve low-threshold lasing and discuss the fabrication tolerances of such a design.

©2008 Optical Society of America

**OCIS codes:** (130.2790) Guided waves; (130.3120) Integrated optics devices; (140.5680) Rare earth and transition metal solid-state lasers.

---

## References and links

1. A. W. Fang, H. Park, O. Cohen, R. Jones, M. J. Paniccia, and J. E. Bowers, "Electrically pumped hybrid AlGaInAs-silicon evanescent laser," *Opt. Express* **14**, 9203-9210 (2006).
2. V. R. Almeida, Q. Xu, C. A. Barrios, and M. Lipson, "Guiding and confining light in void nanostructure," *Opt. Lett.* **29**, 1209-1211 (2004).
3. Q. Xu, V. R. Almeida, R. R. Panepucci, and M. Lipson, "Experimental demonstration of guiding and confining light in nanometer-size low-refractive-index material," *Opt. Lett.* **29**, 1626-1628 (2004).
4. C. A. Barrios and M. Lipson, "Electrically driven silicon resonant light emitting device based on slot-waveguide," *Opt. Express* **13**, 10092-10101 (2005).
5. F. Ning-Ning, J. Michel, and L. C. Kimerling, "Optical field concentration in low-index waveguides," *IEEE J. Quantum Electron.* **42**, 885-890 (2006).
6. J. T. Robinson, C. Manolatou, C. Long, and M. Lipson, "Ultrasmall mode volumes in dielectric optical microcavities," *Phys. Rev. Lett.* **95**, 143901 (2005).
7. E. Burstein and C. Weisbuch, eds. *Confined electrons and photons*, (Plenum Press: New York, NY, 1995).
8. T. D. Visser, H. Blok, B. Demeulenaere, and D. Lenstra, "Confinement factors and gain in optical amplifiers," *IEEE J. Quantum Electron.* **33**, 1763-1766 (1997).
9. C. A. Barrios, K. B. Gylfason, B. Sánchez, A. Griol, H. Sohlström, M. Holgado, and R. Casquel, "Slot-waveguide biochemical sensor," *Opt. Lett.* **32**, 3080-3082 (2007).
10. F. Dell'Olio and V. M. Passaro, "Optical sensing by optimized silicon slot waveguides," *Opt. Express* **15**, 4977-4993 (2007).
11. H. Kogelnik, *Theory of optical waveguides*, in *Guided-wave optoelectronics*, T. Tamir, ed., (Springer Verlag: Berlin, 1990). p. 7.
12. L. A. Coldren and S. W. Corzine, *Diode lasers and photonic integrated circuits* (J. Wiley & Sons, New York, NY, 1995).
13. C. Pollock and M. Lipson, *Integrated photonics* (Kluwer Academic, Norwell, MA, 2003).
14. J. Haes, B. Demeulenaere, R. Baets, D. Lenstra, T. D. Visser, and H. Blok, "Difference between TE and TM modal gain in amplifying waveguides: Analysis and assessment of two perturbation approaches," *Opt. Quantum Electron.* **29**, 263-273 (1997).
15. J. D. Jackson, *Classical electrodynamics*. 3rd ed (John Wiley & Sons, Inc., Hoboken, NJ, 1999).
16. H. A. Haus, *Waves and fields in optoelectronics* (Prentice-Hall, Englewood Cliffs, NJ, 1984).
17. L. D. Landau and E. M. Lifshitz, *Electrodynamics of continuous media* (Pergamon Press, Reading, MA, 1960).

18. G. J. Veldhuis, O. Parriaux, H. J. W. M. Hoekstra, and P. V. Lambeck, "Sensitivity enhancement in evanescent optical waveguide sensors," *J. Lightwave Technol.* **18**, 677-682 (2000).
19. R. Perahia, O. Painter, V. Moreau, and R. Colombelli, "Design of quantum cascade lasers for intra-cavity sensing in the mid infrared," (in preparation).
20. A. E. Siegman, *Lasers* (University Science Books, Sausalito, CA, 1986).
21. J. T. Robinson, L. Chen, and M. Lipson, "On-chip gas detection in silicon optical microcavities," *Opt. Express* **16**, 4296-4301 (2008).

## 1. Introduction

A critical photonic component yet to be demonstrated on a silicon-based platform is an electrically pumped device with optical gain for amplification or lasing. Achieving this optical gain in a silicon-based device is extremely challenging since silicon is an indirect band-gap semiconductor and therefore an inefficient photon source. Hybrid silicon devices based on direct band-gap III-V materials bonded to silicon photonic elements present an interim solution [1], however, the reliance on a wafer bonding step prohibits a high throughput fabrication process possible with a silicon-based process.

One possible configuration for silicon-based gain is the recently proposed slot waveguide design [2, 3]. In this configuration a low-index gain material such as Er-doped SiO<sub>2</sub> or Er-doped Si<sub>3</sub>N<sub>4</sub> can be inserted into one [4] or multiple [5] thin slots between two silicon rails. Electrical excitation of the gain material could be achieved by passing a tunneling current through the slot-region.

One key advantage of this configuration is the large optical field enhancement in the slot-region due to the boundary conditions imposed on the electric field normal the slot interface [6]. Since the normal electric displacement ( $D = \epsilon E$ ) must be continuous across the interface, the electric field in the slot waveguide is enhanced by the ratio of the dielectric constant of silicon to that of the slot material. In semiconductor materials this enhancement can be as large as one order of magnitude.

Typically waveguide gain is assumed to be proportional to the percentage of the guided mode power which overlaps with the gain medium; however, this is not true for high-index contrast waveguides due to the large electric field discontinuities at dielectric interfaces. This discrepancy results from Fermi's Golden Rule which states the electric field of an electromagnetic wave, not the power, determines the emission rate for an excited state [7] (and consequently the modal gain).

In standard low-index-contrast waveguides, optical gain and power confinement are considered proportional based on the following arguments. For electromagnetic plane waves in homogenous media the magnetic field  $\mathbf{H}$  can be written in terms of the electric field  $\mathbf{E}$  and the impedance of the material according to:

$$\mathbf{H} = \frac{c\epsilon}{n} (\hat{\mathbf{e}}_z \times \mathbf{E}), \quad (1)$$

where  $\hat{\mathbf{e}}_z$  is a unit vector along the direction of propagation (which we have chosen to be the  $z$ -direction) and  $n$  is the index of refraction of the material. This is often written in the form relating the major components of the electric and magnetic fields (for a TM mode in this case)[8]:

$$E_y = \frac{-\omega\mu_0}{\beta} H_x, \quad (2)$$

where  $\beta$  is the propagation constant defined as  $\beta \equiv 2\pi\bar{n}/\lambda$ . Based on these relationships the electric field energy, and waveguide power stored in a given region can be used interchangeably since they differ only by a constant. In this case the percentage of power overlapping the gain medium can be used to calculate the resulting modal gain, and it is often assumed that the same can be said for waveguide modes.

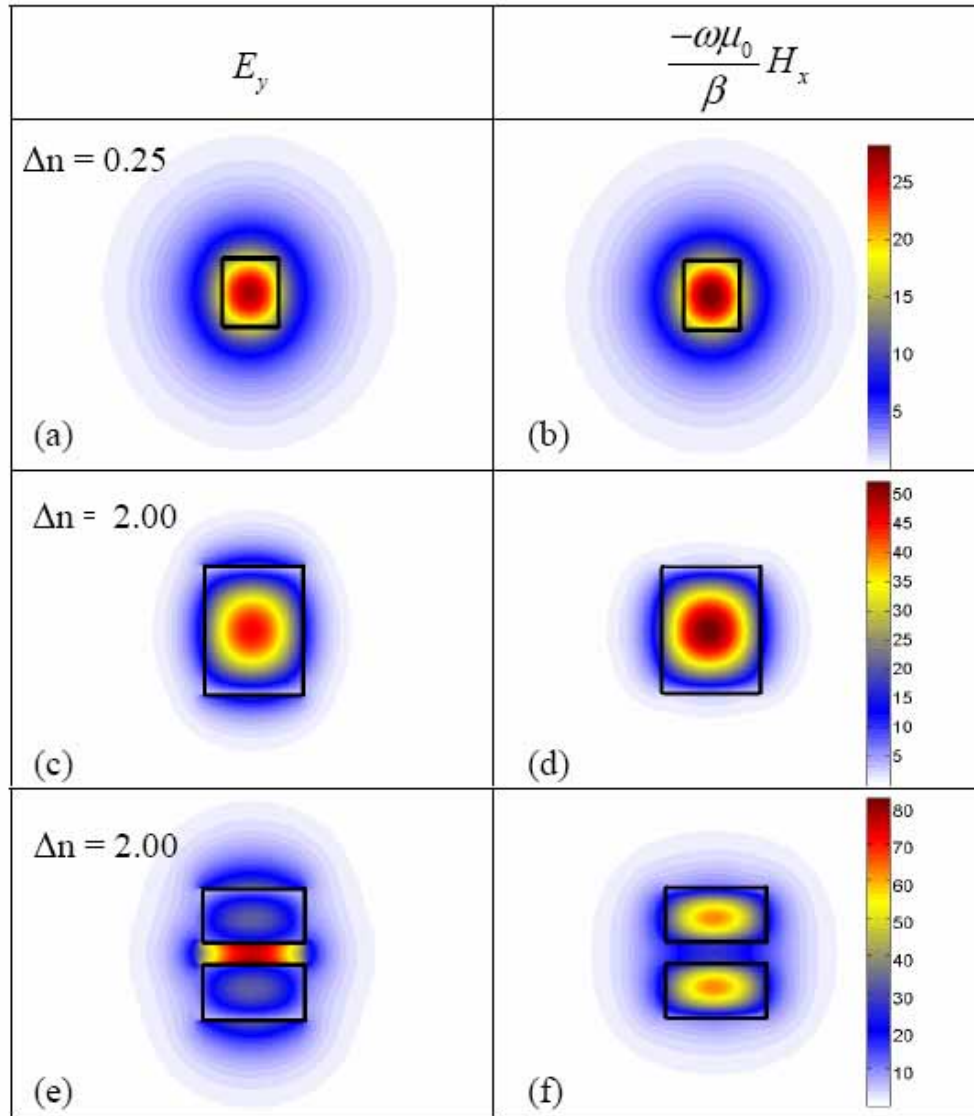


Fig. 1. Fundamental TM modes at a wavelength of  $1.5 \mu\text{m}$  for waveguides  $500 \text{ nm}$  wide and  $600 \text{ nm}$  tall. All modes are normalized to unit power. The high-index material ( $n=3.5$ ) is outlined in black. The waveguides are clad with  $n=3.25$  for (a) and (b) and  $n=1.5$  for (c)-(f).

The first and second columns show  $E_y$  and  $\frac{-\omega\mu_0}{\beta} H_x$  respectively, plotted on the same color scale. The two fields become increasingly dissimilar as more electric field is concentrated at high-index-contrast boundaries.

For high-index-contrast waveguides, however, the linear relationships between the electric and magnetic fields (Eqs. (1) and (2)) do not hold since they must satisfy different boundary conditions. This is shown in Fig. 1. For low-index-contrast waveguides, Eqs. (1) and (2) are close approximations. Figures 1(a) and 1(b) shows the fundamental TM mode with an index difference of  $0.25$  between the core and cladding. We see close agreement in the magnitude and spatial profiles of these two fields. However, as the index-contrast is increased to  $2.5$  (Fig. 1(c) and (d)) there is a noticeable difference between  $E_y$  and  $\frac{-\omega\mu_0}{\beta} H_x$ . Notice that  $E_y$  must

be *continuous* across the dielectric interfaces to the left and right of the waveguide, and *discontinuous* across the top and bottom interfaces. The  $H_x$  on the other hand must be continuous across all interfaces since the magnetic susceptibility is the same in all regions. This leads to noticeable differences between the electric and magnetic field magnitudes and profiles. This difference becomes dramatic when the peak of the electric field is placed at a dielectric discontinuity as is the case for slot waveguides (Figs. 1(e) and 1(f)).

The strong difference between the spatial distribution of the electric and magnetic fields in high index contrast is the reason that power confinement is no longer a relevant quantity when calculating gain in high-index-contrast waveguides. This issue is also present when calculating the sensitivity of waveguides to changes in refractive index. Several previous papers have overcome this problem by either determining waveguide sensitivity empirically [9] or by introducing correction factors [10], however, there is little discussion as to the origin of the correction factors.

In this paper we derive from first principles the appropriate confinement factors and figures of merit for modal gain in high-index-contrast waveguides. We show explicitly that the modal gain is dependent on two quantities: the group velocity and the electric field energy confinement in the slot region. The lasing threshold however is independent of the group velocity and determined only by the electric field energy confinement. We also show that in some instances decreasing the width of the slot can decrease the lasing threshold despite the reduction of gain material. This counter-intuitive result can be understood as the increased emission rate for material in narrow slots [6] overcoming the reduction in volume of gain material. Additionally we show that the percentage of power confined to the slot region (sometimes used as a confinement factor) can incorrectly predict the modal gain in high-index-contrast waveguides.

## 2. Confinement factor for high-index-contrast waveguides

To rigorously calculate gain in high-index-contrast waveguides we derive from first principles a proportionality constant (known as a confinement factor  $\Gamma$ ) which relates bulk material gain ( $g_b$ ) to the modal gain ( $g_m$ ) in a guiding structure:

$$\Gamma \equiv g_m / g_b, \quad (3)$$

where  $g_m$  and  $g_b$  have units of inverse length. The bulk material gain can be determined from the magnitude of the electric field for a plane wave propagating along the z-direction through the gain medium:

$$|E(z)|^2 = |E_0|^2 e^{g_b z} \quad (4)$$

To calculate the effective confinement factor for a given waveguide mode profile, we begin with an expression for the electric field of a guided mode propagating along the z-direction. This can be written as the sum of all three vector components of the electric field using Einstein summation notation:

$$\mathbf{E}(x, y, z) = \hat{\mathbf{e}}_j E_{j0} \Psi_j(x, y) e^{i(\alpha x - \tilde{\beta} z)}, \quad (5)$$

where  $\hat{\mathbf{e}}$  is the polarization vector,  $\Psi$  is the cross sectional mode profile, and  $\tilde{\beta}$  is the complex propagation constant defined as

$$\tilde{\beta} \equiv k_0 (\bar{n}_r + i\bar{n}_i), \quad (6)$$

where  $k_0$  is the angular wavenumber in free space, and  $\bar{n}_r$  and  $\bar{n}_i$  are the real and imaginary parts of the effective index respectively. By writing Eq. (5) in the same form as Eq. (4) we can see that the modal gain is determined by the complex propagation constant. From Eq. (6) we can then write the gain of the guided mode in terms of the imaginary part of the effective index:

$$g_m = 2 \operatorname{Im}\{\tilde{\beta}\} = 2k_0 \bar{n}_i. \quad (7)$$

Similarly we can write the bulk material gain in terms of the imaginary part of refractive index of the active gain material:

$$g_b = 2k_0 n_{Ai}. \quad (8)$$

Expressing gain in this form allows us to treat it as a perturbation to the refractive index of the waveguide. We can now calculate the modal gain by introducing a small imaginary part to the refractive index ( $\Delta n_{Ai}$ ) in a given active region ( $A$ ) and solve for the complex propagation constant of the guided mode. This can be performed using variational methods [11]:

$$\Delta \tilde{\beta} = \frac{\omega \iint_{\infty} \Delta \tilde{\epsilon} |\mathbf{E}|^2 dx dy}{\frac{1}{2} \iint_{\infty} \operatorname{Re}\{\mathbf{E} \times \mathbf{H}^*\} \cdot \hat{\mathbf{e}}_z dx dy}, \quad (9)$$

where  $\Delta \tilde{\epsilon} = (n_A + i\Delta n_{Ai})^2$ . According to Eqs. (6)-(8) this can be written in the form:

$$g_m = \left[ \frac{n_A c \epsilon_0 \iint_A |\mathbf{E}|^2 dx dy}{\iint_{\infty} \operatorname{Re}\{\mathbf{E} \times \mathbf{H}^*\} \cdot \hat{\mathbf{e}}_z dx dy} \right] g_b. \quad (10)$$

Here  $c$  is the speed of light in vacuum, the integral in the numerator is carried out only over the area of the active gain region (since this is where  $\Delta \tilde{\epsilon} \neq 0$ ), and the integral in the denominator is carried out over the entire cross section of the mode. We recognize the term in the brackets as the proportionality constant in Eq. (3) and therefore we can express the confinement factor as:

$$\Gamma = \frac{n_A c \epsilon_0 \iint_A |\mathbf{E}|^2 dx dy}{\iint_{\infty} \operatorname{Re}\{\mathbf{E} \times \mathbf{H}^*\} \cdot \hat{\mathbf{e}}_z dx dy}. \quad (11)$$

Note that as expected the stimulated emission rate (and thus the gain) depends on the intensity of the field which is proportional to  $|\mathbf{E}|^2$ . Since this term is normalized to unit power, the confinement factor can be thought of as the amount of intensity overlapping the gain medium per unit input power. Note that most previous derivations of this confinement factor err by incorrectly substituting the electric for magnetic field in attempts to simplify the expression. This is commonly written as [12-14]:

$$\frac{1}{2} \iint \operatorname{Re}\{\mathbf{E} \times \mathbf{H}^*\} \cdot \hat{\mathbf{e}}_z dx dy = \frac{1}{2} \frac{\beta}{\omega \mu_0} \iint |\mathbf{E}|^2 dx dy, \quad (12)$$

and thus Eq. (11) could be written as the percentage of power or intensity confined to the active region. However, as shown in Section 1, **the expression in Eq. (12) is not valid** for high-index-contrast waveguides since it is based on the relationship for plane waves in homogeneous media that  $\mathbf{H} = \frac{c}{n} (\hat{\mathbf{e}}_z \times \mathbf{E})$  [15].

The expression for the confinement factor (Eq. (9)) can be simplified into the product of two terms: one related to the group velocity, and the other related to the confinement of the energy density of the electric field. The energy stored per unit length ( $U/l$ ) in a dielectric waveguide can be written as [15]:

$$U/l = \frac{1}{2} \iint_{\infty} \epsilon |\mathbf{E}|^2 dx dy. \quad (13)$$

Note that here we have neglected material dispersion when writing the stored energy per unit length. To account for material dispersion one should replace epsilon with  $d(\omega\epsilon)/d\omega$  in Eq. (11) [16, 17]. If silicon is the most dispersive material, the error introduced by making this approximation is less than 7% at a wavelength of 1.55 microns. The group velocity of the mode ( $v_g$ ) describes the speed with which energy flows through a given cross section. Therefore we can write the power flux through a given cross section of the waveguide as:

$$\frac{1}{2} \iint \text{Re}\{\mathbf{E} \times \mathbf{H}^*\} \cdot \hat{\mathbf{e}}_z dx dy = v_g \frac{1}{2} \iint \epsilon |\mathbf{E}|^2 dx dy \quad (14)$$

Using the definition of group index ( $n_g \equiv c/v_g$ ) we substitute Eq. (14) into Eq. (11) and rewrite the confinement factor as:

$$\Gamma = \frac{n_g \iint_A \epsilon |\mathbf{E}|^2 dx dy}{n_A \iint_{\infty} \epsilon |\mathbf{E}|^2 dx dy} \equiv \frac{n_g}{n_A} \gamma_A. \quad (15)$$

We see from the simplified expression for the confinement factor that the modal gain can be defined as the product of a term related to the group index and a term related to the confinement of the electric field energy density. The first term can be thought of as a confinement in time since increasing the real part of the group index relative to the bulk index has the effect of slowing the propagation of the guided mode. Therefore for a given waveguide length, light can spend more time in the gain media resulting in an enhancement of the modal gain per unit length. The second term represents the spatial confinement of the energy density to the active region of the waveguide which we define as:

$$\gamma_A \equiv \frac{\iint_A \epsilon |\mathbf{E}|^2 dx dy}{\iint_{\infty} \epsilon |\mathbf{E}|^2 dx dy}. \quad (16)$$

Since this term can be as large as 1 we see that the total confinement factor in Eq. (15) can be larger than 1 if the group index is larger than the bulk refractive index. This means that it is possible to achieve more gain per unit length in a guided structure than would be possible in bulk. This phenomenon has been noted before for modal absorption [18] and results from the fact that light spends more time in a structure with a large group index, and thus interacts more with the gain material per unit length.

### 3. Numerical verification of analytical results

To verify our expression for the confinement factor (Eq. (13)) we use numerical methods to calculate the relationship between material gain and modal gain and compare it to the analytical results. Since the material gain can be expressed in terms of an imaginary part of the dielectric constant, we can simulate material gain in a given waveguide region by adding an imaginary component to the dielectric constant and calculating the propagation constant of the guided mode using a finite difference mode solver. The imaginary part of this complex propagation constant can then be written in terms of the modal gain according to Eq. (7). This relationship between the modal gain and material gain is the definition of the confinement factor Eq. (3) and should match the derived expression Eq. (15).

We numerically calculate the modal gain according to the waveguide geometry and the corresponding fundamental TM mode as shown in Figure 2(a) and 2(b) respectively. The waveguide geometry consists of two high index rails 500 nm wide and 250 nm tall separated by a horizontal slot 50 nm tall. For simplicity we use a wavelength of 1.5  $\mu\text{m}$  and 3.5 and 1.5 for the high and low refractive indices respectively. This is approximately the index contrast between Si and SiO<sub>2</sub>. Figure 2(b) shows the fundamental TM mode calculated using a Matlab-based finite difference mode solver. We simulate material gain by introducing an imaginary

part of the dielectric constant to the low-index slot region. For each value of material gain we use the finite difference mode solver to calculate the complex propagation constant and calculate the corresponding modal gain according to Eq. (7).

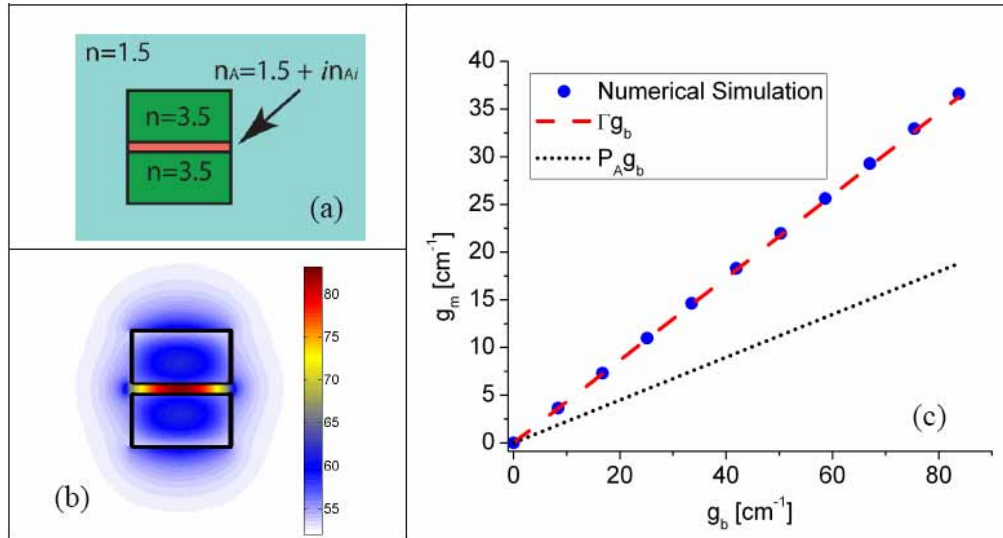


Fig. 2. Numerical study of modal gain. (a) Schematic of slot waveguide with gain material defined by an imaginary component of the refractive index confined to the slot region (pink). (b) Major field component of the fundamental TM mode for the same structure as (a) calculated using a finite difference mode solver. (c) Circles show the modal gain ( $g_m$ ) calculated from the complex effective index of the fundamental TM mode as determined using a finite difference mode solver. Material gain is added via the imaginary part of the refractive index in the slot. Dashed line shows the modal gain calculated according to Eq. (3) based on the confinement factor  $\Gamma$  determined from the zero-gain mode profile from Eq. (15). Dotted line shows the product of the power in the active gain region ( $P_A$ ) and the material gain. We see that the confinement factor proposed in this paper correctly predicts the modal gain simulated numerically, while the power confinement greatly underestimates the simulated modal gain.

By plotting the numerically calculated modal gain ( $g_m$ ) versus material gain ( $g_b$ ) in Fig. 1(c) we show excellent agreement with the analytically calculated confinement factor. The slope of the line  $g_m$  versus  $g_b$  (circles in Fig. 1(c)) represents the confinement factor according to Eq. (3). We also calculate the confinement factor  $\Gamma$  based on Eq. (15) and the calculated TM mode in Fig. 1(b). We plot  $\Gamma g_b$  as the dashed line in Fig. 1(c). As expected, our calculated confinement factor agrees very well with the relationship between the modal and material gain from numerical simulations. The difference between these two factors (0.4328 from Eq. (15) and 0.4368 from the numerical simulations) is less than 1%. To highlight the difference between this confinement factor and the confinement of power to the gain medium we also plot on this graph  $P_A g_b$  where we define the power in the active region as:

$$P_A \equiv \frac{\iint_A \text{Re}\{\mathbf{E} \times \mathbf{H}^*\} \cdot \mathbf{e}_z dx dy}{\iint_{-\infty}^{\infty} \text{Re}\{\mathbf{E} \times \mathbf{H}^*\} \cdot \mathbf{e}_z dx dy}. \quad (17)$$

We see from Fig. 1(c) that the modal gain of a slot waveguide is substantially larger than would be expected from the percentage of power confined to the gain region. As discussed in Section 2, this enhanced modal gain results from both the large group index as well as the increased electric field energy density in the slot. The electric field energy density is underestimated using the  $\mathbf{H}$  field (See Figs. 1(e) and 1(f)).

#### 4. Minimizing the lasing threshold

One of the primary interests in these structures is achieving lasing, therefore it is important to identify which factors aid in reaching the condition that the modal gain exceeds the modal loss. Since material gain was written as a positive imaginary part of the material's refractive index, similarly, material loss can be written as a negative imaginary part of the refractive index. The modal loss can then be determined following the same derivation in Section 1. The result is that the modal loss ( $\alpha_m$ ) is related to the bulk material loss ( $\alpha_b$ ) by

$$\alpha_m = \frac{n_g}{n_b} \gamma_b \alpha_b, \quad (18)$$

where  $n_b$  is the refractive index of the bulk material and  $\gamma_b$  is the energy density confinement in the material similar to Eq. (16). In general there will be several loss mechanisms which can be written as sum of terms of the form Eq. (18). To achieve lasing, the threshold condition requires the modal gain per unit length be greater than the modal loss per unit length:

$$n_g \frac{\gamma_A}{n_A} g_b - n_g \sum_i \frac{\gamma_i}{n_i} \alpha_i > 0. \quad (19)$$

We see immediately that the group index can be divided out of Eq. (19). This is because increasing  $n_g$  increases the time it takes light to propagate through the waveguide which increases both the gain *and* loss per unit length equally.

We see from the lasing threshold condition (Eq. (19)) that increasing the group index will not help one reach the lasing threshold despite that fact that the gain per unit length increases. While above and below the lasing threshold the net modal gain depends on the confinement factor  $\Gamma$ , we see from Eq. (19) that the lasing threshold itself is determined only by the confinement of the electric field energy density ( $\gamma_A$ ). Although  $\gamma_A$  is generally larger than the power confinement in the slot, it is always less than or equal to 1. Therefore the lowest lasing threshold for these structures is limited by the bulk material gain. An identical result can be derived by analyzing resonant cavities. In that case  $\gamma_A$  relates the material to modal gain per unit *time* [19].

Based on the threshold condition in Eq. (19) we can define a new figure of merit which represents how easily lasing can be achieved in a waveguide. Since in practice the modal loss  $\alpha_m$  is often an experimentally measured parameter with units of inverse length, we can substitute this measured quantity into Eq. (19) and rewrite the lasing threshold condition as:

$$g_b > \frac{\alpha_m}{\Gamma}. \quad (20)$$

This quantity  $\frac{\alpha_m}{\Gamma}$  is a useful figure of merit since it is equal to the minimum bulk material gain needed to reach the lasing threshold in the waveguide. Because the group index cancels out in Eq. (18), this figure of merit can be directly compared for waveguides of different geometries to determine which can achieve lasing with the lowest material gain coefficient.

#### 5. Scaling behavior of gain versus slot thickness

While narrow slots enjoy greater local field enhancement, they also contain less gain material. Therefore the important question arises as to how the total gain in these structures depends on the slot thickness. As the width of the slot becomes increasingly narrow, the magnitude of the electric field increases until it reaches its maximum determined by the difference between dielectric constants in the high and low index region. This results in a greater stimulated (and spontaneous) emission rate of the material in the slot region [6]. According to the laser rate

equations this should result in larger modal gain coefficients [20]. However, as the slot becomes increasingly narrow the area of the active region decreases. Therefore although the gain material is “working harder” there is less matter contributing to the gain. Thus it is important to understand how these competing phenomena affect the lasing threshold.

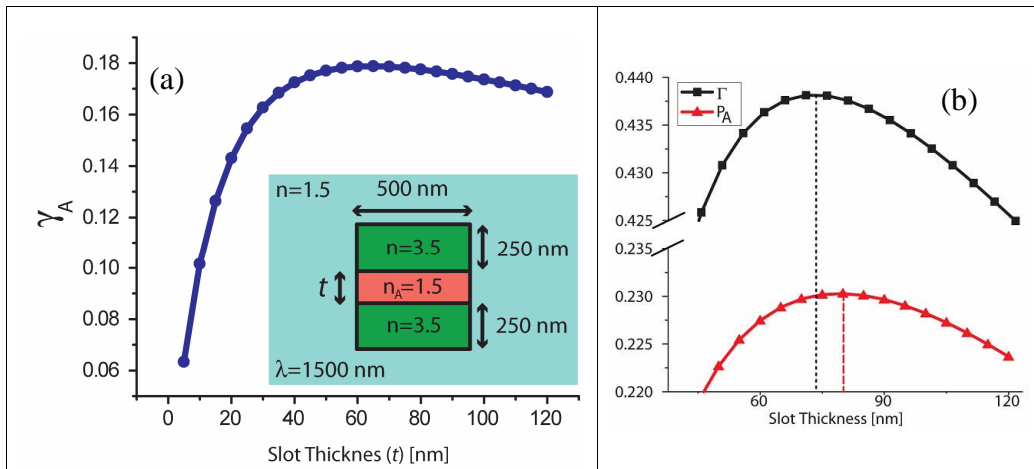


Fig. 3. (a). The spatial confinement factor  $\gamma_A$  plotted as a function of slot thickness  $t$ , where the gain region is defined as the slot (pink region in inset) between the high-index rails (green). Narrow slots result greater emission rates of gain material while thicker slots provide more material which contributes to the gain. The peak in  $\gamma_A$  near a slot width of 60 nm indicates the condition where the combination of enhanced emission rate and volume of gain material result in the lowest lasing threshold. (b). The total confinement factor ( $\Gamma$ ) (squares) and power in the slot region ( $P_A$ ) (triangles) as a function of slot width. Dotted and dashed lines mark the slot widths which maximize  $\Gamma$  and  $P_A$  respectively. The discrepancy between these two plots shows that the percentage of power in the gain media is not an accurate indication of either the magnitude or the optimal design for modal gain.

To minimize the lasing threshold we look for a maximum in the spatial confinement factor ( $\gamma_A$ ) as a function of slot thickness which is plotted in Fig. 3(a). The maximum near a slot width of 60 nm illustrates the important point that the tradeoff between emission rate (which *increases* as the slot is narrowed) and material volume (which *decreases* as the slot is narrowed) results in an optimal slot width for minimizing the lasing threshold. Initially, as the slot narrows from 120 nm, the increased emission rate more than compensates for the decrease in volume of gain material, and  $\gamma_A$  increases. Near a thickness of about 50 nm the emission rate begins to saturate as it approaches its maximum value determined by the index contrast between the high and low index regions. After this point, further reduction of the slot thickness decreases the volume of material contributing to the gain without much enhancement of the emission rate, and the result is a sharp drop in  $\gamma_A$ .

As a comparison to previous methods, we plot in Fig. 3(b) the relative power confined in the slot region according to Eq. (17) and show again that slot waveguides outperform expectations based on previous theoretical treatments. We see that *both* the magnitude of the modal gain *and* the optimal geometry are miscalculated using this method. The gain calculated numerically (in agreement with  $\Gamma$ ) is nearly twice as large as would be expected based on the power confined to the slot mode. Additionally, the optimal slot width is miscalculated by more than 10% using power confinement.

## 6. Optimizing slot waveguide geometry

To optimize the dimensions of a slot waveguide for an electrically pumped silicon laser, we apply the principles in the proceeding sections to achieve a waveguide design with a minimal lasing threshold. We estimate that the slot thickness should be no larger than 10 nm in order to achieve electrical injection via tunneling into an oxide-based gain media using bias voltages on the order of volts [4]. Therefore we keep the slot thickness fixed at 10 nm and compute the confinement factors as we vary the height and width of the waveguide. Here we have used the refractive indices of Si (3.48) and SiO<sub>2</sub> (1.46) as the high and low index material respectively, and a wavelength of 1.55 μm. We have assumed that gain only occurs in the slot region. Figures 4(b)–4(d) show respectively the total confinement factor ( $\Gamma$ ), the group index normalized to the slot index ( $n_g/n_A$ ), and the energy density confinement factor ( $\gamma_A$ ) as a function of height and width of the waveguide.

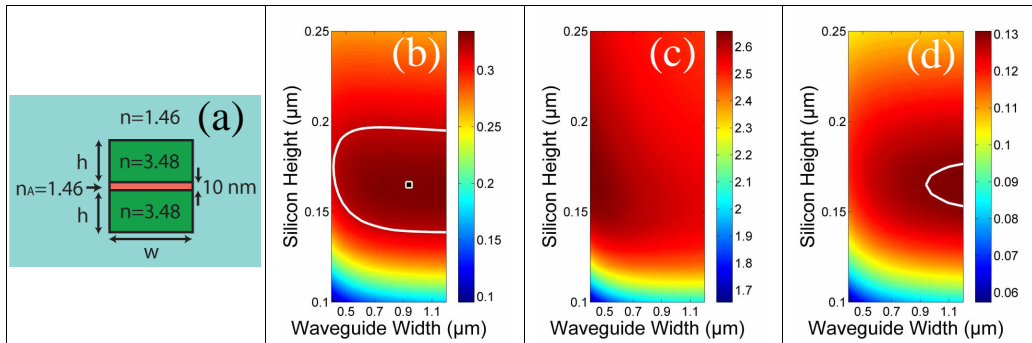


Fig. 4. Optimization of width and height of Si/SiO<sub>2</sub>/Si slot waveguide with a 10 nm thick slot assumed to contain a gain medium. (a) Schematic of slot waveguide. (b) Total confinement factor  $\Gamma$ , proportional to the total modal gain. (c) Group index  $n_g$  divided by the slot index (1.46), which is responsible for the difference between the lasing threshold and modal gain. (d) Electric field energy confinement  $\gamma_A$ , inversely proportional to the lasing threshold. The maximum total modal gain is marked by the square in (a). The white contour shows the region which corresponds to a 5% change from the maximum values of  $\Gamma$  and  $\gamma_A$ .

We see in Fig. 4(b) that the maximum modal gain for a 10 nm thick slot occurs near a waveguide width of 940 nm and a height of 340 nm (marked by the square) and has a value  $\Gamma = 0.336$ . Both the energy density and group index peak near a waveguide height of 340 nm. As the width of the waveguide is increased, the energy density in the slot region (and thus the net gain) increases. The group index, on the other hand, decreases with increasing waveguide width. These competing parameters result in a maximum  $\Gamma$  near a width of about 940 nm.

In contrast to the modal gain, with a fixed slot thickness, the minimal lasing threshold (determined by  $\gamma_A$ ) shows no well-defined optimum. This is because the lasing threshold will scale only with the energy density confinement. The value of  $\gamma_A$  (Fig. 4(d)) increases monotonically with waveguide width and asymptotically approaches the value for an infinitely wide slab waveguide, which we calculate to have a maximum of  $\gamma_A = 0.137$  for a waveguide height of 340 nm.

We see from Fig. 4 that the optimal device geometry is relatively insensitive to variation in waveguide dimensions. Around the optimal design, variations of approximately  $\pm 50$  nm in the total height and width of the waveguide result in changes in the confinement factors of less than 5%. This allows the device performance to be relatively unaffected by size variations which can occur during fabrication.

## 7. Discussion and conclusions

We have shown that some commonly applied metrics are not appropriate for determining gain in high-index-contrast waveguides, and from first principles developed several figures of merit to characterize waveguide structures for gain. In particular we have shown that the concept of power confinement to the gain region significantly miscalculates the gain experienced by the waveguide mode. Instead we have shown that the true confinement factor which determines gain per unit length results from the combination of group index and confinement of the electric field energy to the gain region. These terms can combine and in some cases exceed unity meaning that one can achieve greater gain per unit length than would be possible in the bulk material. The lasing threshold on the other hand only depends on the percentage of electric field energy in the gain region. To account for this we have introduced a new figure of merit to describe the suitability of a waveguide to achieve low-threshold lasing. This figure of merit is the experimentally measured propagation loss divided by the confinement factor introduced in this paper. The evaluation of this ratio determines the minimal material gain required to achieve lasing in the waveguide structure.

Additionally we have applied our analysis to the design of slot waveguide structures. We have shown that the lasing threshold has a minimum for a particular slot width and increases dramatically as the slot is made thinner. Also we have shown that gain characteristics of the waveguides are fairly insensitive to variations in overall waveguide dimensions.

Since the confinement factors presented here were derived from perturbation theory, they can be applied to other phenomena in high-index-contrast waveguides including refractive index sensing. In deriving the confinement factors presented here we have studied gain as a perturbation of the imaginary part of the refractive index over a given region of the guided mode. The same formalism holds true for perturbations to the real part of the refractive index and therefore the confinement factors for gain presented in the paper can also be used as confinement factors for refractive index sensing [10, 18] and have shown good agreement with experiment [21].

In summary, this work provides the qualitative and quantitative analysis necessary in developing high-index-contrast waveguides for applications such as amplification and lasing.

## Acknowledgments

The authors gratefully acknowledge Thomas L. Koch for his helpful discussions and Christina Manolatu for the use of her finite difference mode solver. Research support is gratefully acknowledged from the National Science Foundation Center on Materials and Devices for Information Technology Research (CMDITR), DMR-0120967, the National Science Foundation's CAREER Grant No. 0446571, and the U.S. Air Force MURI program on "Electrically-Pumped Silicon-Based Lasers for Chip-Scale Nanophotonic Systems" supervised by Dr. Gernot Pomrenke.